Broken-Symmetry States in N≥2 Landau Levels in GaAs/AlGaAs Quantum Wells: A Brief Review

Xiaojun Fu * and Zedong Yang

Posted Date: 18 August 2025

doi: 10.20944/preprints202508.1229.v1

Keywords: broken-symmetry states;two-dimensional electron systems;quantum Hall effects

 doi:10.20944/preprints202508.1229.v1

Article

Broken-Symmetry States in $N \geq 2$ Landau Levels in GaAs/AlGaAs Quantum Wells: A Brief Review

Xiaojun Fu * and Zedong Yang

Independent Researcher
* Correspondence: xfuumn@gmail.com

Abstract

In a clean two-dimensional electron systems, the interplay between electron-electron interactions and disorder gives rise to emergent collective phases, including anisotropic stripe phases and re-entrant integer quantum Hall phases (bubble phases) in high Landau levels ($N \geq 2$). These phases, first observed in GaAs/AlGaAs quantum wells, represent broken-symmetry states whose detailed nature continues to be intensively explored. New models incorporating quantum and thermal fluctuations have refined our understanding of these phases. Recent experimental advances have revealed intricate behaviors such as stripe orientation transitions, nematic-to-smetic transition, and anomalous nematic states, and hidden quantum Hall stripes. This review synthesizes the progress in probing broken-symmetry states in $N \geq 2$ Landau levels in GaAs/AlGaAs quantum wells, highlighting both consensus and open challenges in the field.

Keywords: broken-symmetry states; two-dimensional electron systems; quantum Hall effects

1. Introduction

The quantum Hall effect in two-dimensional electron systems (2DES) has long served as a paradigm for exploring strongly correlated electron physics in low dimensions. In conventional settings, the integer and fractional quantum Hall effect [1,2] emerge in the lowest Landau levels due to Landau quantization and many-body correlations. However, in higher Landau levels ($N \geq 2$), a new class of collective states appears — markedly distinct from conventional quantum Hall liquids. Chief among these are the anisotropic stripe phases and re-entrant integer quantum Hall phases (bubble phases) [3,4], which arise from the competition between long-range repulsive and short-range attractive components of Coulomb interaction in partially filled high Landau levels.

Stripe phases, also referred to as unidirectional charge density waves, manifest in transport experiments as pronounced anisotropy in longitudinal resistance near half-integer filling factors (e.g., $\nu = 9/2, 11/2, 13/2$). In contrast, bubble phases - consisting of localized clusters of electrons - yield reentrant integer quantum Hall states at nearby fillings. Both types of order break translational symmetry and are stabilized in ultra-clean 2DES such as GaAs/AlGaAs heterostructures, where disorder is sufficiently weak to allow the formation of long-range electronic crystalline order [5,6].

The theoretical framework for understanding these phases was initially established through Hartree-Fock calculations, which predicted the emergence of stripe and bubble ground states due to exchange interactions at high orbital indices [7,8]. Subsequent developments have enriched this picture, introducing concepts from classical liquid crystal physics (such as nematic and smectic order) [9], as well as quantum fluctuation and pinning effects [10–12]. These have led to a more nuanced understanding of the role of symmetry breaking, collective modes, and phase transitions in these systems.

On the experimental side, a variety of sophisticated techniques—including microwave resonance spectroscopy, nonlinear transport, and tilted-field measurements—have been employed to characterize

 doi:10.20944/preprints202508.1229.v1

the properties of stripe and bubble phases [13–16]. Recent experiments have revealed rich phenomenology such as stripe reorientation transitions, nematic-to-smetic phase transition, anomalous nematic states, and hidden quantum Hall phases, that reflect the interaction between charge order and disorder [17–23].

This review synthesizes recent advances in the study of broken-symmetry phases in GaAs/AlGaAs quantum wells. We aim to provide a brief overview of research progress, identify areas of consensus, and highlight open questions that continue to drive research in this rapidly evolving field.

2. Theoretical Background

2.1. Hartree-Fock Approximation

The emergence of broken-symmetry phases in high Landau levels ($N \geq 2$) was first theoretically predicted through pioneering Hartree–Fock calculations by Koulakov, Fogler, and Shklovskii [7,8]. Within this framework, the effective electron–electron interaction acquires a peculiar "boxlike" form due to screening and the oscillatory structure of Landau-level wavefunctions. This interaction strongly favors inhomogeneous charge distributions over uniform states, leading to the stabilization of complex charge density wave phases.

At half-filling of a high Landau level, the Hartree–Fock solution predicts a unidirectional charge density modulation, or "stripe phase," in which the electron density alternates periodically between two adjacent integer filling factors. For instance, at $\nu = 9/2$, the system organizes into parallel stripes of $\nu = 4$ and $\nu = 5$ regions, producing a quasi–one-dimensional electronic texture. The period of these stripes was found to be on the order of the cyclotron radius, a direct consequence of the nodal structure of higher Landau level wavefunctions. Such stripe ordering naturally explains the striking transport anisotropy observed in experiments, where conductivity is high along the stripe direction but strongly suppressed perpendicular to it.

Away from half-filling, Hartree–Fock predicts a transition from stripe order to "bubble phases," where the excess or deficit electrons cluster into circular droplets containing multiple electrons. These droplets then crystallize into a triangular Wigner-like lattice, minimizing the Coulomb repulsion. The number of electrons per bubble depends on the filling fraction, with larger bubbles forming as one moves further away from half-filling.

Importantly, the Hartree–Fock description becomes quantitatively accurate only for Landau levels with large orbital index ($N \geq 2$). In the lowest and first excited Landau levels ($N = 0, 1$), quantum fluctuations are sufficiently strong to destabilize such charge density wave

phases, giving rise instead to fractional quantum Hall liquids. Thus, the emergence of stripe and bubble phases is a distinctive feature of high-N Landau levels, reflecting the interplay between the form of the effective interaction and the reduced role of quantum fluctuations.

2.2. Role of Quantum and Thermal Fluctuations

While Hartree–Fock theory successfully captures the basic structure of charge density wave phases, it neglects quantum and thermal fluctuations that crucially influence phase stability and dynamics. Beyond mean-field, numerical studies using density matrix renormalization group and exact diagonalization have demonstrated the competition between broken-symmetry states and alternative phases such as isotropic liquids and Wigner crystals, particularly in the presence of disorder or at finite temperature [24–26].

Quantum fluctuations have been directly linked to the stabilization of nematic liquid crystalline phases, which preserve orientational order while destroying long-range translational order [9,27]. These nematics exhibit soft Goldstone modes associated with broken rotational symmetry, offering a natural explanation for the strong transport anisotropy observed experimentally. Field-theoretical approaches further describe their critical behavior, predicting non-Fermi-liquid scaling and emergent gauge fields near the nematic transition [28,29].

 doi:10.20944/preprints202508.1229.v1

Disorder plays a dual role: it suppresses long-range order but simultaneously enables experimental detection of charge density wave phases through pinning. Elastic models adapted from classical charge density waves describe a collective pinning regime in which resonance frequencies emerge from the interplay between elasticity and disorder [12,30]. More recent theories emphasize rare strong pinning centers, showing that even weak disorder can localize collective modes, generate glassy dynamics, and account for metastability and hysteresis observed in bubble phases [31].

The analogy with classical smectic liquid crystals motivates the study of topological defects, including dislocations and disclinations, as drivers of melting transitions. The proliferation of such defects can destroy long-range anisotropy, particularly at elevated temperatures or under strong drive [32–34]. Incorporating these defects into theoretical models yields universal scaling predictions for nonlinear transport and pinning resonance linewidths [35,36].

Finally, stripe and nematic phases can also be viewed as manifestations of a Pomeranchuk instability of the Fermi surface - an instability toward spontaneous distortion without breaking translational symmetry [37,38]. This perspective connects quantum Hall nematics to a broader family of symmetry-breaking electronic states in correlated materials such as cuprates and iron-based superconductors.

3. Experimental Foundations

3.1. Two-Dimensional Electron Systems in GaAs/AlGaAs Heterostructures

Experimental studies of GaAs/AlGaAs heterostructures have provided compelling evidence for the existence of stripe and bubble phases in high Landau levels. These observations rely on ultra–high-mobility two-dimensional electron systems, typically with mobility exceeding $\mu \gtrsim 10^7$ cm^{2}V^{-1}s^{-1}, which enable the formation of fragile charge density wave states at millikelvin temperatures.

Figure 1a illustrates the band edge and charge density profiles in an ultra–high-mobility GaAs quantum well. Because GaAs has a smaller band gap and lower conduction band energy than AlGaAs, it forms a natural quantum well, with conducting carriers supplied by donor impurities. In early devices, Si atoms were doped into the AlGaAs barriers, so that electrons in the GaAs well experienced only a weak scattering potential from ionized donors. In modern structures, however, silicon dopants are placed in extremely narrow (3 nm) GaAs doping wells that are sandwiched between 2 nm AlAs barriers [Figure 1b]. In this design, charge transfers not only to the primary two-dimensional electron gas in the 30 nm GaAs quantum well, but also to the *X*-point band edge of the AlAs barriers. Because the heavy-mass *X* electrons exhibit very low mobility, they contribute negligibly to parallel conduction [39]. With an appropriate doping level, they do not appear in magnetotransport measurements [40].

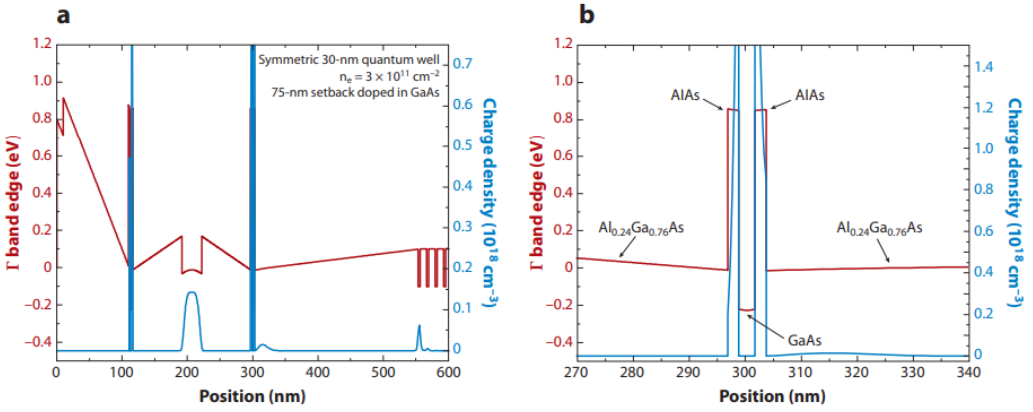

Figure 1. Band edge and charge density profiles in a GaAs quantum well. (a) A two-dimensional electron gas resides in a 30 nm GaAs quantum well confined by Al0.24Ga0.76As barriers. Silicon impurities are introduced in the center of a narrow 3 nm GaAs doping well, sandwiched between 2 nm AlAs layers. (b) Γ-point conduction band edge and free charge density in the immediate vicinity of the doping well. Figure adapted from Ref. [40].

The doping-well architecture provides two key advantages. First, the exchange of Al and Si atoms in AlGaAs barriers can generate DX centers, which act as strong scattering centers [41]. By placing

 doi:10.20944/preprints202508.1229.v1

silicon in GaAs instead of AlGaAs, such DX centers are eliminated. Second, the excess carriers in the AlAs layers help screen the potential of parent ions, thereby reducing remote impurity scattering of the two-dimensional electron system (2DES) [39,40]. Together, these effects allow the realization of exceptionally high-quality 2DESs suitable for observing fragile correlated states.

3.2. Stripe Phases and Transport Anisotropy

The hallmark of stripe phases is a pronounced anisotropy in longitudinal resistance near half-integer filling factors, most notably at $\nu = 9/2$, $11/2$, and higher [3,4]. As illustrated in Figure 2, magnetotransport measurements reveal a strong directional dependence: R_{xx} exhibits a peak, while R_{yy} shows a dip at half filling factors. In contrast, the Hall resistance is not quantized in these broken-symmetry states. The anisotropy emerges below $T \approx 100$ mK. Because the high-resistance axis consistently aligns with the crystalline direction $\hat{x} \equiv \langle 1\bar{1}0 \rangle$, the stripes themselves are inferred to lie along the orthogonal direction $\hat{y} \equiv \langle 110 \rangle$. Transport is therefore easy (low resistance) along the stripes and hard (high resistance) across them. Beyond direct current transport, anisotropy has also been observed through microwave pinning resonance [42] and surface acoustic wave propagation [43,44].

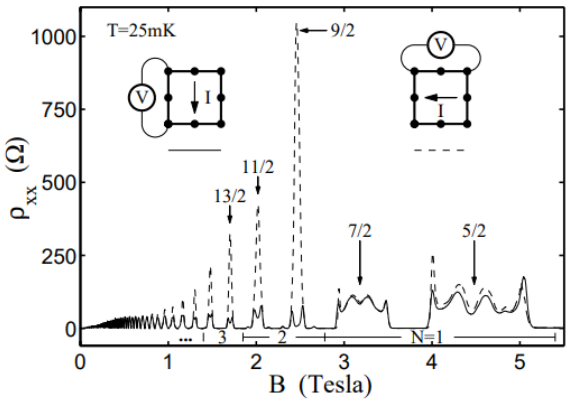

Figure 2. One of the first observations on quantum Hall stripes. Magnetotransport along two orthogonal directions show a great anisotropy identified by a peak in R_{xx} and a dip in R_{yy} at half-filled filling factors $\nu = 9/2, 11/2, 13/2$,... The figure is taken from Ref. [3].

In nearly all reported cases, the hard axis lies along $\langle 1\bar{1}0 \rangle$. The few exceptions — where it switches to $\langle 110 \rangle$ — have been found only in samples with unusually high electron density [45,46]. More recent work, however, indicates that even at densities as large as $n_e \geq 4.0 \times 10^{11}\text{cm}^{-2}$, the hard axis remains along $\langle 1\bar{1}0 \rangle$ [47]. The persistence of this preferred orientation strongly suggests the presence of an intrinsic symmetry-breaking field within the semiconductor heterostructure. Yet, despite nearly two decades of intensive study [16,46,48], the microscopic origin of this native symmetry breaker remains unresolved.

3.3. Reentrant Integer Quantum Hall Phases

Shortly after the Hartree–Fock prediction of charge density wave phases, experimental signatures of bubble crystals were reported [3,4]. Because they are pinned by disorder, bubble phases are insulating, and their transport characteristics resemble those of nearby integer filling factors, leading to so-called reentrant integer quantum Hall states. Figure 3 presents one of the earliest observations: near $\nu \approx 4.25$ and 4.75, both R_{xx} and R_{yy} are strongly suppressed, while R_H remains quantized at integer values. Subsequent experiments have reinforced the bubble interpretation through nonlinear transport [49,50], microwave pinning resonance [13,51], onset temperature studies [52], surface acoustic wave propagation [43,44], and screening efficiency measurements [53].

 doi:10.20944/preprints202508.1229.v1

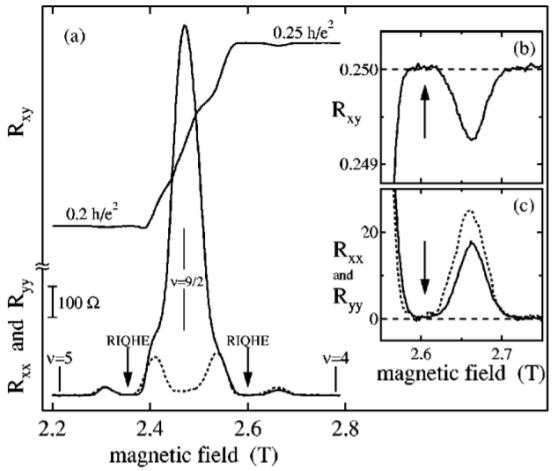

Figure 3. One of the first observations of reentrant integer quantum Hall states (quantum Hall bubbles). Near $\nu \approx 4.25$ and 4.75, both R_{xx} and R_{yy} are small, and R_H exhibits the integer quantum hall states at $T \approx 50$ mK. The figure is taken from Ref. [49].

From a theoretical standpoint, the number of distinct reentrant integer quantum Hall states is expected to increase with Landau level index, since larger N allows more electrons per bubble. Early experimental evidence, however, did not support this trend: the same number of reentrant integer quantum Hall states was observed in both the $N = 2$ and $N = 3$ Landau levels. One possibility is that multiple bubble configurations (with different numbers of electrons per cluster) coexist within a single reentrant integer quantum Hall state, though such distinctions are difficult to resolve experimentally. Only recently have two independent studies provided evidence for this scenario, successfully distinguishing between two- and three-electron bubbles in the $N = 3$ Landau level [54,55].

4. Emerging Phenomena and Open Questions

4.1. Stripe Reorientation Under In-Plan Magnetic Field $B_{||}$

Shortly after the discovery of quantum Hall stripe phases, it was established that an in-plane magnetic field $B_{||}$ can reorient the stripes, as evidenced by a reversal of the easy and hard transport directions [56,57]. A variety of other perturbations can also reorient stripes, including heterostructure design [46], weak density modulation [58], spin and charge distribution [59], mechanical strain [16], and electric current [60]. Early experiments consistently found that $B_{||}$ favors stripes oriented perpendicular to its direction, an effect attributed to orbital coupling between cyclotron motion and the confinement potential, which alters electron–electron interactions and the cohesive energy of stripe phases [61,62]. While initial theories predicted a universal perpendicular alignment in single-subband systems [61], later calculations showed that parallel alignment could arise in thicker two-dimensional electron gases [62].

More recent experiments reveal that the $B_{||}$-induced reorientation is far more complex than initially understood, with multiple reorientations occurring as $B_{||}$ is increased. At moderate fields, stripes typically rotate perpendicular to $B_{||}$, but at larger $B_{||}$ a second type of reorientation favors alignment parallel to the field. Figure 4 illustrates this phenomenology. In zero in-plane field near $\nu = 9/2$, native stripes are aligned along $\hat{y}$, producing strong transport anisotropy with $R_{xx} \gg R_{yy}$ [Figure 4(a)]. When a modest in-plane field is applied parallel to these stripes ($B_{||} = B_y$), they rotate into the $\hat{x}$ direction, i.e., perpendicular to $B_{||}$ [Figure 4(b)]. Unexpectedly, further increasing B_y leads to a second reorientation: at $\theta_y = 46^\circ$, the stripes rotate back to their native $\hat{y}$ direction, now aligned parallel to $B_{||}$ [Figure 4(c)]. A similar reorientation sequence occurs when $B_{||}$ is applied perpendicular to the native stripes ($B_{||} = B_x$), with alignment again parallel to $B_{||}$ at $\theta_x = 42^\circ$ [Figure 4(d)]. Importantly, the two reorientation mechanisms display distinct dependencies: the perpendicular-alignment field B_c

 doi:10.20944/preprints202508.1229.v1

is largely insensitive to spin index σ and decreases slightly with Landau level index N, whereas the parallel-alignment fields B_c' grow with N and are markedly smaller for spin index $\sigma = +1/2$ than for $\sigma = -1/2$ [17].

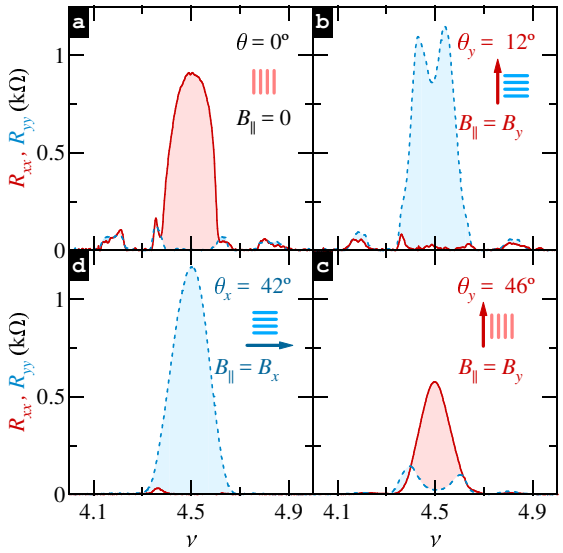

Figure 4. Figure 4.1: R_{xx} (solid line) and R_{yy} (dotted line) versus ν at (a) $\theta = 0°$, (b) $B_{||} = B_y$ and $\theta_y = 12°$, (c) $B_{||} = B_y$ and $\theta_y = 46°$, and (d) $B_{||} = B_x$ and $\theta_x = 42°$. Figure adapted from Ref. [17].

These results indicate a nontrivial coupling between the native symmetry-breaking potential (which fixes the zero-field stripe direction) and the $B_{||}$-induced anisotropy. Unlike the additive-energy picture invoked in early models [61,62], recent work suggests that $B_{||}$ modifies the anisotropy energy landscape in a way consistent with wavefunction-deformation scenarios, effectively shifting rather than simply adding to the native symmetry-breaking potential [18]. Temperature-dependent studies further reveal that both parallel- and perpendicular-aligned stripes show similar thermal suppression of anisotropy, though perpendicular stripes tend to persist over a broader filling-factor range. At still higher $B_{||}$, even more complex behavior emerges, including a third reorientation, with the sequence and number of transitions depending sensitively on sample details. Tuning electron density within a single sample using an *in situ* gate [63] unifies this diversity, demonstrating that density plays a central role in the competition between native and $B_{||}$-induced orienting mechanisms [19]. Together, these findings reveal a much richer interplay between orbital coupling, spin, Landau level structure, and the native symmetry-breaking potential than previously recognized, motivating more refined theoretical approaches to stripe energetics in the presence of strong in-plane fields.

4.2. Possible Electronic Liquid Crystalline States

Possible lectronic liquid crystalline phases developed at half fillings are classified by the specific symmetries they break [64]. The nematic phase breaks rotational symmetry while retaining translational invariance [29,64–66], giving rise to strong transport anisotropy without long-range periodic density modulations. The smectic phase—essentially a unidirectional charge density wave—breaks rotational symmetry as well as translational symmetry in one direction [64,67–70]. At the next level of symmetry breaking, the stripe crystal (or bubble crystal) breaks translational symmetry in both directions, forming a fully ordered electronic solid [12,32,64,67,71–73]. At elevated temperatures or in samples with stronger disorder, the system remains an isotropic electronic liquid with all symmetries intact. Figure 4 schematically summarizes these phases. Experimentally, most evidence to date has supported the nematic state as the ground state near half filling. More recent experiments in ultra-clean samples at electron temperatures below 30 mK suggest a richer phase sequence: an isotropic-to-nematic transition at intermediate temperatures, followed at still lower temperatures by a nematic-to-smectic crossover [20]. Supporting evidence includes (i) a non-monotonic temperature dependence of R_{xx},

 doi:10.20944/preprints202508.1229.v1

which turns downward at the lowest temperatures in a manner consistent with enhanced inter-stripe scattering in the smectic; (ii) nonlinear I–V characteristics indicative of partial depinning; and (iii) large low-frequency noise with $1/f^{\alpha}$ spectra and telegraph-like fluctuations, reminiscent of defect dynamics in conventional charge density waves. Crucially, these signatures are absent or strongly suppressed in more disordered samples, highlighting the extreme fragility of the smectic state.

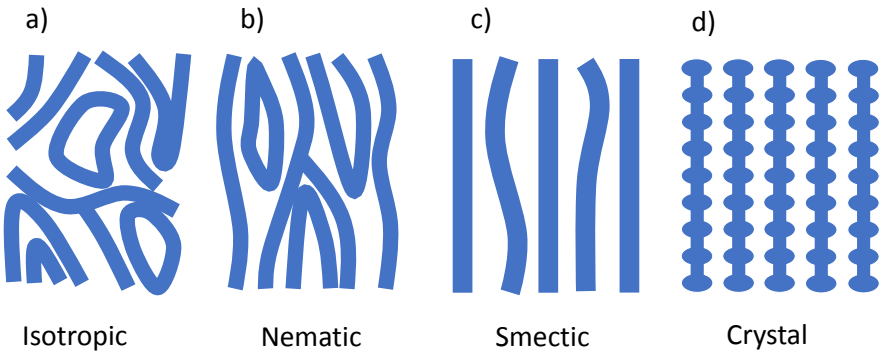

Figure 5. Cartoon of electronic liquid crystal phases at half- filling. (a) Isotropic liquid (b) Nematic liquid crystal. (c) Smectic liquid crystal (d) Anisotropic stripe crystal. Blue regions indicate high filling factor (i.e., high density of electron guiding centers) and white regions indicate low filling factor. Figure adapted from Ref. [20].

4.3. Anomalous Nematic States

A recent experiment reports on anomalous nematic states, which are distinguished from quantum Hall stripe phases by minima (maxima) in R_{xx} (R_{yy}) and plateau-like features in R_H in half-filled $N \geq 3$ Landau levels [21]. The global maxima (minima) in R_{xx} (R_{yy}) occur away from half filling, at $\delta\nu \approx \pm 0.08$, where the resistance anisotropy ratio attains its maximal value, as shown in Figure 6. Remarkably, all these features emerge at temperatures considerably lower than the onset temperature of quantum Hall stripes, indicating a possible transition to a new phase.

The response of anomalous nematic states to in-plane magnetic fields $B_{\|} = B_x$ and $B_{\|} = B_y$ has also been investigated [23]. The immediate effect of $B_{\|}$ is to transform the minimum (maximum) in R_{xx} (R_{yy}) at half filling into a maximum (minimum), to eliminate the plateau in R_H, and to restore the ratio R_{xx}/R_{yy} to values consistent with quantum Hall stripe phases. Remarkably, anomalous nematic states respond to $B_{\|}$ in essentially the same manner when $B_{\|}$ is applied along either the $\hat{x} \equiv \langle 1\bar{1}0 \rangle$ or the $\hat{y} \equiv \langle 110 \rangle$ direction; in both cases, the revived quantum Hall stripe phase is aligned along its native $\langle 110 \rangle$ crystal axis. This is in contrast to the effect of $B_{\|}$ on quantum Hall stripe phases, which respond very differently to B_x and B_y and persist to much higher $B_{\|}$ values. These observations indicate that a modest $B_{\|} \approx 0.5$ T is sufficient to tip the delicate balance between the anomalous nematic states and the quantum Hall stripe phases in favor of the latter—a finding that should be considered in theoretical efforts to explain the origin of anomalous nematic states.

 doi:10.20944/preprints202508.1229.v1

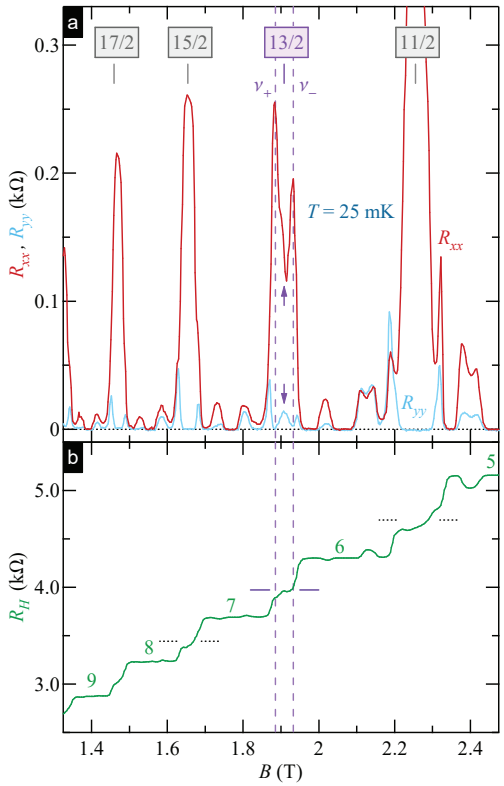

Figure 6. (a) R_{xx} and R_{yy} versus B at $T \approx 25$ mK. Half-integer ν are marked by 15/2, 13/2, and 11/2. The R_{xx} minimum and the R_{yy} maximum at $\nu \approx 13/2$ are indicated by $\uparrow$ and $\downarrow$, respectively. Dashed vertical lines are drawn at $\nu_\pm = 6.5 \pm 0.08$. (b) Hall resistance R_H versus B. Solid horizontal lines, drawn at $2R_K/13$, mark a plateau-like feature near $\nu = 13/2$, while dashed horizontal lines are drawn at $2R_K/11$ ($\nu = 11/2$) and $2R_K/15$ ($\nu = 15/2$), where $R_K \equiv h/e^2 = 25812.80745\ \Omega$ is the von Klitzing constant. Figure adapted from Ref. [21].

4.4. Hidden Quantum Hall Stripes

While quantum Hall stripes have been robustly observed in GaAs-based systems, their exploration in other material platforms remains limited, in part because the symmetry-breaking mechanisms enabling macroscopic alignment may be absent [48]. A recent theoretical development [74] predicted the existence of hidden quantum Hall stripe phases—states sharing the underlying stripe order of quantum Hall stripes but exhibiting isotropic resistivity ($\rho_{xx} \approx \rho_{yy}$) independent of filling factor, as shown in Figure 7. These phases occupy the intermediate regime between conventional quantum Hall stripes at lower half-filled Landau levels and isotropic liquids at higher filling factors, the latter characterized by a $1/\nu$ resistivity scaling [75,76]. The hidden quantum Hall stripe phase is expected to appear when scattering processes suppress directional diffusion anisotropy without destroying the stripe order, thereby eliminating the transport anisotropy signature that typically reveals quantum Hall stripe formation.

Hidden quantum Hall stripe phases have now experimentally confirmed the existence of in $Al_xGa_{1-x}As/Al_{0.24}Ga_{0.76}As$ quantum wells with extremely low Al mole fractions ($x < 10^{-3}$) [22]. By tuning alloy disorder through controlled Al incorporation, a phase diagram was mapped in the conductivity–filling factor plane, identifying the boundaries between quantum Hall stripe phases, hidden quantum Hall stripe phases, and isotropic phases. They found that the hidden quantum Hall stripe phases exhibit a filling-factor-independent resistivity plateau over a broad range, with stability enhanced by short-range alloy scattering. The extracted quantum Hall stripe density of states was significantly lower than the Hartree–Fock prediction, suggesting the need for refined theoretical treatments.

 doi:10.20944/preprints202508.1229.v1

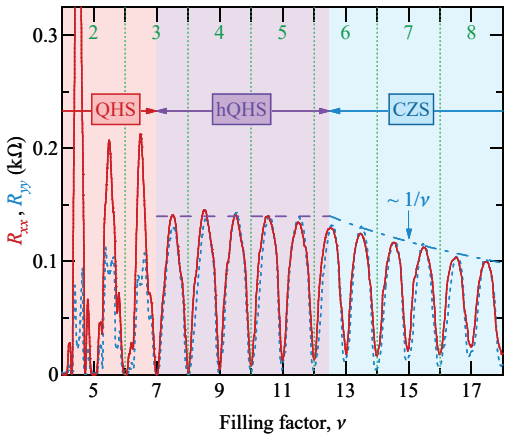

Figure 7. Longitudinal resistances R_{xx} (solid line) and R_{yy} (dotted line) as a function of the filling factor ν measured in sample B. Gap centers between spin-resolved Landau levels are labeled by $N = 2, 3, \ldots$ at the top axis ($\nu = 2N + 1$). The conventional quantum Hall stripe (QHS) phase ($R_{xx} > R_{yy}$) and the isotropic phase confirmed by Coleridge, Zawadski, and Sachrajda (CZS) [75] ($R_{xx} \approx R_{yy} \propto \nu^{-1}$) occur at half-integer $\nu = 9/2, 11/2, 13/2$ and at $\nu = 27/2, 29/2, \ldots$, respectively. The hidden quantum Hall stripe phase (hQHS) is identified at intermediate half-integer filling factors, $\nu = 15/2, \ldots, 25/2$, where the resistance is isotropic and ν-independent. The characteristic ν^0 (ν^{-1}) dependence of the isotropic resistance in the hQHS (isotropic) phase is marked by dashed (dash-dotted) line. Figure adapted from Ref. [22].

Importantly, the study also explains the absence of hidden quantum Hall stripe phases phases in ultraclean GaAs quantum wells: in these systems, the two boundaries between hidden quantum Hall stripes and quantum Hall stripe phases, and between hidden quantum Hall stripe phases and isotropic phases collapses, leaving no stability window. This experimental confirmation of hidden quantum Hall stripe phases not only extends the taxonomy of quantum Hall stripe states but also broadens the range of materials and conditions under which stripe physics can be probed. Given that electron nematicity and stripe ordering are central to understanding correlated phenomena in systems ranging from high-T_c superconductors [77,78] to moiré superlattices [79,80], the hidden quantum Hall stripe regime offers a unique platform for studying the interplay between disorder, symmetry breaking, and emergent electronic order in low-dimensional systems.

5. Conclusions

In high Landau levels ($N \geq 2$) of two-dimensional electron systems, the competition between electron–electron interactions and disorder leads to the emergence of broken symmetry states including anisotropic stripe phases and reentrant integer quantum Hall phases. In this review, we have outlined the theoretical framework, key experimental observations, and recent advances in the study of these broken symmetry states in GaAs/AlGaAs quantum wells. While Hartree–Fock theory captures the essential phase structure, experiments now reveal a far richer landscape, such as nematic–smectic crossovers, multiple $B_{\parallel}$-induced reorientations, and anomalous nematic states. These findings highlight the need for continued investigation, both experimental and theoretical, to unravel the roles of quantum and thermal fluctuations, disorder, and symmetry-breaking mechanisms in shaping the phase diagram of high Landau levels.

Author Contributions: X. F. and Z. Y. prepared and revised the manuscript. Both authors have read and agreed to the published version of the manuscript.

Funding: This research received no external funding

Institutional Review Board Statement: Not applicable.

Informed Consent Statement: Not applicable.

Data Availability Statement: Not applicable.

 doi:10.20944/preprints202508.1229.v1

Acknowledgments: Not applicable.

Conflicts of Interest: The authors declare no conflicts of interest.

Abbreviations

The following abbreviations are used in this manuscript:

2DES	Two-dimensional electron systems
QHS	Quantum Hall stripes
hQHS	Hidden quantum Hall stripes

References

1. von Klitzing, K.; Dorda, G.; Pepper, M. New Method for High-Accuracy Determination of the Fine-Structure Constant Based on Quantized Hall Resistance. *Phys. Rev. Lett.* **1980**, *45*, 494.
2. Tsui, D.C.; Stormer, H.L.; Gossard, A.C. Two-Dimensional Magnetotransport in the Extreme Quantum Limit. *Phys. Rev. Lett.* **1982**, *48*, 1559.
3. Lilly, M.P.; Cooper, K.B.; Eisenstein, J.P.; Pfeiffer, L.N.; West, K.W. Evidence for an Anisotropic State of Two-Dimensional Electrons in High Landau Levels. *Phys. Rev. Lett.* **1999**, *82*, 394.
4. Du, R.R.; Tsui, D.C.; Stormer, H.L.; Pfeiffer, L.N.; Baldwin, K.W.; West, K.W. Strongly anisotropic transport in higher two-dimensional Landau levels. *Solid State Commun.* **1999**, *109*, 389.
5. Eisenstein, J.P.; MacDonald, A.H. Bose–Einstein condensation of excitons in bilayer electron systems. *Nature (London)* **2004**, *432*, 691.
6. Fradkin, E.; Kivelson, S.A.; Lawler, M.J.; Eisenstein, J.P.; Mackenzie, A.P. Nematic Fermi Fluids in Condensed Matter Physics. *Annu. Rev. Condens. Matter Phys.* **2010**, *1*, 153. https://doi.org/10.1146/annurev-conmatphys-070909-103925.
7. Koulakov, A.A.; Fogler, M.M.; Shklovskii, B.I. Charge density wave in two-dimensional electron liquid in weak magnetic field. *Phys. Rev. Lett.* **1996**, *76*, 499.
8. Fogler, M.M.; Koulakov, A.A.; Shklovskii, B.I. Ground state of a two-dimensional electron liquid in a weak magnetic field. *Phys. Rev. B* **1996**, *54*, 1853.
9. Fradkin, E.; Kivelson, S.A. Liquid-crystal phases of quantum Hall systems. *Phys. Rev. B* **1999**, *59*, 8065. https://doi.org/10.1103/PhysRevB.59.8065.
10. Wexler, C.; Dorsey, A.T. Disclination unbinding transition in quantum Hall liquid crystals. *Phys. Rev. B* **2001**, *64*, 115312. https://doi.org/10.1103/PhysRevB.64.115312.
11. Mulligan, M.; Nayak, C.; Kachru, S. Isotropic to anisotropic transition in a fractional quantum Hall state. *Phys. Rev. B* **2010**, *82*, 085102. https://doi.org/10.1103/PhysRevB.82.085102.
12. Fertig, H.A. Unlocking Transition for Modulated Surfaces and Quantum Hall Stripes. *Phys. Rev. Lett.* **1999**, *82*, 3693–3696. https://doi.org/10.1103/PhysRevLett.82.3693.
13. Lewis, R.M.; Ye, P.D.; Engel, L.W.; Tsui, D.C.; Pfeiffer, L.N.; West, K.W. Microwave Resonance of the Bubble Phases in 1/4 and 3/4 Filled High Landau Levels. *Phys. Rev. Lett.* **2002**, *89*, 136804.
14. Chen, Y.; Lewis, R.M.; Engel, L.W.; Tsui, D.C.; Ye, P.D.; Pfeiffer, L.N.; West, K.W. Microwave Resonance of the 2D Wigner Crystal around Integer Landau Fillings. *Phys. Rev. Lett.* **2003**, *91*, 016801.
15. Samkharadze, N.; Schreiber, K.A.; Gardner, G.C.; Manfra, M.J.; Fradkin, E.; Csathy, G.A. Observation of a transition from a topologically ordered to a spontaneously broken symmetry phase. *Nat. Phys.* **2016**, *12*, 191.
16. Koduvayur, S.P.; Lyanda-Geller, Y.; Khlebnikov, S.; Csathy, G.; Manfra, M.J.; Pfeiffer, L.N.; West, K.W.; Rokhinson, L.P. Effect of Strain on Stripe Phases in the Quantum Hall Regime. *Phys. Rev. Lett.* **2011**, *106*, 016804. https://doi.org/10.1103/PhysRevLett.106.016804.
17. Shi, Q.; Zudov, M.A.; Watson, J.D.; Gardner, G.C.; Manfra, M.J. Reorientation of quantum Hall stripes within a partially filled Landau level. *Phys. Rev. B* **2016**, *93*, 121404. https://doi.org/10.1103/PhysRevB.93.121404.
18. Shi, Q.; Zudov, M.A.; Watson, J.D.; Gardner, G.C.; Manfra, M.J. Evidence for a new symmetry breaking mechanism reorienting quantum Hall nematics. *Phys. Rev. B* **2016**, *93*, 121411. https://doi.org/10.1103/PhysRevB.93.121411.
19. Shi, Q.; Zudov, M.A.; Qian, Q.; Watson, G.C.; Manfra, M.J. Reorientation of stripe phases by in-plane magnetic fields in a tunable-density two-dimensional electron gas. *submitted* **2016**.

 doi:10.20944/preprints202508.1229.v1

20. Qian, Q.; Nakamura, J.; Fallahi, S.; Gardner, G.C.; Manfra, M.J. Possible nematic to smectic phase transition in a two-dimensional electron gas at half-filling. *Nature Communications* **2017**, *8*, 1536. https://doi.org/10.1038/s41467-017-01810-y.
21. Fu, X.; Shi, Q.; Zudov, M.A.; Gardner, G.C.; Watson, J.D.; Manfra, M.J.; Baldwin, K.W.; Pfeiffer, L.N.; West, K.W. Anomalous Nematic States in High Half-Filled Landau Levels. *Phys. Rev. Lett.* **2020**, *124*, 067601. https://doi.org/10.1103/PhysRevLett.124.067601.
22. Fu, X.; Huang, Y.; Shi, Q.; Shklovskii, B.I.; Zudov, M.A.; Gardner, G.C.; Manfra, M.J. Hidden Quantum Hall Stripes in $Al_xGa_{1-x}As/Al_{0.24}Ga_{0.76}As$ Quantum Wells. *Phys. Rev. Lett.* **2020**, *125*, 236803. https://doi.org/10.1103/PhysRevLett.125.236803.
23. Fu, X.; Shi, Q.; Zudov, M.A.; Gardner, G.C.; Watson, J.D.; Manfra, M.J.; Baldwin, K.W.; Pfeiffer, L.N.; West, K.W. Anomalous nematic state to stripe phase transition driven by in-plane magnetic fields. *Phys. Rev. B* **2021**, *104*, L081301. https://doi.org/10.1103/PhysRevB.104.L081301.
24. Rezayi, E.H.; Haldane, F.D.M.; Yang, K. Charge-Density-Wave Ordering in Half-Filled High Landau Levels. *Phys. Rev. Lett.* **1999**, *83*, 1219. https://doi.org/10.1103/PhysRevLett.83.1219.
25. Shibata, N.; Yoshioka, D. Ground-state phase diagram of two-dimensional electrons in higher Landau levels. *Physical Review Letters* **2001**, *86*, 5755–5758.
26. Shibata, N.; Yoshioka, D. Stripe and bubble phases in the quantum Hall regime. *Journal of the Physical Society of Japan* **2003**, *72*, 664–667.
27. Kivelson, S.A.; Fradkin, E.; Emery, V.J. Electronic liquid-crystal phases of a doped Mott insulator. *Nature* **1998**, *393*, 550–553.
28. Metlitski, M.A.; Sachdev, S. Quantum phase transitions of metals in two spatial dimensions. I. Ising-nematic order. *Phys. Rev. B* **2010**, *82*, 075127.
29. Sun, K.; Fregoso, B.M.; Lawler, M.J.; Fradkin, E. Fluctuating Stripes in Strongly Correlated Electron Systems and the Nematic–Smectic Quantum Phase Transition. *arXiv preprint arXiv:0805.3526* **2008**.
30. Fogler, M.M.; Huse, D.A. Collective pinning of charge-density waves in high Landau levels. *Physical Review B* **2000**, *62*, 7553–7570.
31. Nandkishore, R.; Huse, D.A.; Sondhi, S.L. Rare region effects dominate weakly disordered three-dimensional Dirac points. *Physical Review B* **2012**, *86*, 045128.
32. MacDonald, A.H.; Fisher, M.P.A. Quantum theory of quantum Hall smectics. *Phys. Rev. B* **2000**, *61*, 5724–5733. https://doi.org/10.1103/PhysRevB.61.5724.
33. Abanin, D.A.; Levitov, L.S. Transport in strongly correlated two-dimensional electron fluids. *Physical Review B* **2010**, *82*, 035428.
34. Cooper, K.B.; Lilly, M.P.; Eisenstein, J.P.; Jungwirth, T.; Pfeiffer, L.N.; West, K.W. An Investigation of Orientational Symmetry-Breaking Mechanisms in High Landau Levels. *Solid State Commun.* **2001**, *119*, 89.
35. Schöll, E. *Nonlinear spatio-temporal dynamics and chaos in semiconductors*; Cambridge University, Cambridge, 2001.
36. Fogler, M.M. Dynamics of disordered stripe phases in high Landau levels. *Physical Review B* **2002**, *66*, 153304.
37. Oganesyan, V.; Kivelson, S.A.; Fradkin, E. Quantum Theory of a Nematic Fermi Fluid. *Phys. Rev. B* **2001**, *64*, 195109.
38. Quintanilla, J.; et al.. Asymptotic Pomeranchuk instability of Fermi liquids in half-filled Landau levels. *Scientific Reports* **2023**.
39. Friedland, K.J.; Hey, R.; Kostial, H.; Klann, R.; Ploog, K. *Phys. Rev. Lett.* **1996**, *77*, 4616.
40. Manfra, M.J. Molecular Beam Epitaxy of Ultra-High-Quality AlGaAs/GaAs Heterostructures: Enabling Physics in Low-Dimensional Electronic Systems. *Annu. Rev. Condens. Matter Phys.* **2014**, *5*, 347–373. https://doi.org/10.1146/annurev-conmatphys-031113-133905.
41. Chadi, D.J.; Chang, K.J. Energetics of DX-center formation in GaAs and $Al_xGa_{1-x}As$ alloys. *Phys. Rev. B* **1989**, *39*, 10063–10074. https://doi.org/10.1103/PhysRevB.39.10063.
42. Sambandamurthy, G.; Lewis, R.M.; Zhu, H.; Chen, Y.P.; Engel, L.W.; Tsui, D.C.; Pfeiffer, L.N.; West, K.W. Observation of Pinning Mode of Stripe Phases of 2D Systems in High Landau Levels. *Phys. Rev. Lett.* **2008**, *100*, 256801. https://doi.org/10.1103/PhysRevLett.100.256801.
43. Msall, M.E.; Dietsche, W. Acoustic measurements of the stripe and the bubble quantum Hall phase. *New Journal of Physics* **2015**, *17*, 043042. https://doi.org/10.1088/1367-2630/17/4/043042.
44. Friess, B.; Peng, Y.; Rosenow, B.; von Oppen, F.; Umansky, V.; von Klitzing, K.; Smet, J.H. Negative permittivity in bubble and stripe phases. *Nature Physics* **2017**, *13*, 1124–1129. https://doi.org/10.1038/nphys4213.

 doi:10.20944/preprints202508.1229.v1

45. Zhu, J.; Pan, W.; Stormer, H.L.; Pfeiffer, L.N.; West, K.W. Density-Induced Interchange of Anisotropy Axes at Half-Filled High Landau Levels. *Phys. Rev. Lett.* **2002**, *88*, 116803. https://doi.org/10.1103/PhysRevLett.88.116803.
46. Pollanen, J.; Cooper, K.B.; Brandsen, S.; Eisenstein, J.P.; Pfeiffer, L.N.; West, K.W. Heterostructure symmetry and the orientation of the quantum Hall nematic phases. *Phys. Rev. B* **2015**, *92*, 115410. https://doi.org/10.1103/PhysRevB.92.115410.
47. Fu, X.; Shi, Q.; Zudov, M.A.; Chung, Y.J.; Baldwin, K.W.; Pfeiffer, L.N.; West, K.W. Quantum Hall stripes in high-density GaAs/AlGaAs quantum wells. *Phys. Rev. B* **2018**, *98*, 205418. https://doi.org/10.1103/PhysRevB.98.205418.
48. Sodemann, I.; MacDonald, A.H. Theory of Native Orientational Pinning in Quantum Hall Nematics. *arXiv:1307.5489* **2013**.
49. Cooper, K.B.; Lilly, M.P.; Eisenstein, J.P.; Pfeiffer, L.N.; West, K.W. Insulating phases of two-dimensional electrons in high Landau levels: Observation of sharp thresholds to conduction. *Phys. Rev. B* **1999**, *60*, 11285. https://doi.org/10.1103/PhysRevB.60.R11285.
50. Wang, X.; Fu, H.; Du, L.; Liu, X.; Wang, P.; Pfeiffer, L.N.; West, K.W.; Du, R.R.; Lin, X. Depinning transition of bubble phases in a high Landau level. *Phys. Rev. B* **2015**, *91*, 115301. https://doi.org/10.1103/PhysRevB.91.115301.
51. Lewis, R.M.; Chen, Y.; Engel, L.W.; Tsui, D.C.; Ye, P.D.; Pfeiffer, L.N.; West, K.W. Evidence of a First-Order Phase Transition Between Wigner-Crystal and Bubble Phases of 2D Electrons in Higher Landau Levels. *Phys. Rev. Lett.* **2004**, *93*, 176808.
52. Deng, N.; Watson, J.D.; Rokhinson, L.P.; Manfra, M.J.; Csáthy, G.A. Contrasting energy scales of reentrant integer quantum Hall states. *Phys. Rev. B* **2012**, *86*, 201301. https://doi.org/10.1103/PhysRevB.86.201301.
53. Villegas Rosales, K.A.; Singh, S.K.; Deng, H.; Chung, Y.J.; Pfeiffer, L.N.; West, K.W.; Baldwin, K.W.; Shayegan, M. Melting phase diagram of bubble phases in high Landau levels. *Phys. Rev. B* **2021**, *104*, L121110. https://doi.org/10.1103/PhysRevB.104.L121110.
54. Fu, X.; Shi, Q.; Zudov, M.A.; Gardner, G.C.; Watson, J.D.; Manfra, M.J. Two- and three-electron bubbles in $Al_xGa_{1-x}As/Al_{0.24}Ga_{0.76}As$ quantum wells. *Phys. Rev. B* **2019**, *99*, 161402. https://doi.org/10.1103/PhysRevB.99.161402.
55. Ro, D.; Myers, S.A.; Deng, N.; Watson, J.D.; Manfra, M.J.; Pfeiffer, L.N.; West, K.W.; Csáthy, G.A. Stability of multielectron bubbles in high Landau levels. *Phys. Rev. B* **2020**, *102*, 115303. https://doi.org/10.1103/PhysRevB.102.115303.
56. Lilly, M.P.; Cooper, K.B.; Eisenstein, J.P.; Pfeiffer, L.N.; West, K.W. Anisotropic States of Two-Dimensional Electron Systems in High Landau Levels: Effect of an In-Plane Magnetic Field. *Phys. Rev. Lett.* **1999**, *83*, 824. https://doi.org/10.1103/PhysRevLett.83.824.
57. Pan, W.; Du, R.R.; Stormer, H.L.; Tsui, D.C.; Pfeiffer, L.N.; Baldwin, K.W.; West, K.W. Strongly Anisotropic Electronic Transport at Landau Level Filling Factor under a Tilted Magnetic Field. *Phys. Rev. Lett.* **1999**, *83*, 820. https://doi.org/10.1103/PhysRevLett.83.820.
58. Mueed, M.A.; Hossain, M.S.; Pfeiffer, L.N.; West, K.W.; Baldwin, K.W.; Shayegan, M. Reorientation of the Stripe Phase of 2D Electrons by a Minute Density Modulation. *Phys. Rev. Lett.* **2016**, *117*, 076803. https://doi.org/10.1103/PhysRevLett.117.076803.
59. Liu, Y.; Kamburov, D.; Shayegan, M.; Pfeiffer, L.N.; West, K.W.; Baldwin, K.W. Spin and charge distribution symmetry dependence of stripe phases in two-dimensional electron systems confined to wide quantum wells. *Phys. Rev. B* **2013**, *87*, 075314. https://doi.org/10.1103/PhysRevB.87.075314.
60. Gores, J.; Gamez, G.; Smet, J.H.; Pfeiffer, L.; West, K.; Yacoby, A.; Umansky, V.; von Klitzing, K. Current-Induced Anisotropy and Reordering of the Electron Liquid-Crystal Phases in a Two-Dimensional Electron System. *Phys. Rev. Lett.* **2007**, *99*, 246402.
61. Jungwirth, T.; MacDonald, A.H.; Smrčka, L.; Girvin, S.M. Field-tilt anisotropy energy in quantum Hall stripe states. *Phys. Rev. B* **1999**, *60*, 15574. https://doi.org/10.1103/PhysRevB.60.15574.
62. Stanescu, T.D.; Martin, I.; Phillips, P. Finite-Temperature Density Instability at High Landau Level Occupancy. *Phys. Rev. Lett.* **2000**, *84*, 1288. https://doi.org/10.1103/PhysRevLett.84.1288.
63. Watson, J.D.; Csáthy, G.A.; Manfra, M.J. Impact of Heterostructure Design on Transport Properties in the Second Landau Level of *In Situ* Back-Gated Two-Dimensional Electron Gases. *Phys. Rev. Applied* **2015**, *3*, 064004. https://doi.org/10.1103/PhysRevApplied.3.064004.
64. Fradkin, E.; Kivelson, S.A. Liquid-crystal phases of quantum Hall systems. *Phys. Rev. B* **1999**, *59*, 8065–8072. https://doi.org/10.1103/PhysRevB.59.8065.

 doi:10.20944/preprints202508.1229.v1

65. Fradkin, E.; Kivelson, S.A.; Manousakis, E.; Nho, K. Nematic Phase of the Two-Dimensional Electron Gas in a Magnetic Field. *Phys. Rev. Lett.* **2000**, *84*, 1982. https://doi.org/10.1103/PhysRevLett.84.1982.
66. Radzihovsky, L.; Dorsey, A.T. Theory of Quantum Hall Nematics. *Phys. Rev. Lett.* **2002**, *88*, 216802. https://doi.org/10.1103/PhysRevLett.88.216802.
67. Yi, H.; Fertig, H.A.; Côté, R. Stability of the Smectic Quantum Hall State: A Quantitative Study. *Phys. Rev. Lett.* **2000**, *85*, 4156–4159. https://doi.org/10.1103/PhysRevLett.85.4156.
68. Barci, D.G.; Fradkin, E.; Kivelson, S.A.; Oganesyan, V. Theory of the quantum Hall Smectic Phase. I. Low-energy properties of the quantum Hall smectic fixed point. *Phys. Rev. B* **2002**, *65*, 245319. https://doi.org/10.1103/PhysRevB.65.245319.
69. Barci, D.G.; Fradkin, E. Theory of the quantum Hall Smectic Phase. II. Microscopic theory. *Phys. Rev. B* **2002**, *65*, 245320. https://doi.org/10.1103/PhysRevB.65.245320.
70. Lawler, M.J.; Fradkin, E. Quantum Hall smectics, sliding symmetry, and the renormalization group. *Phys. Rev. B* **2004**, *70*, 165310. https://doi.org/10.1103/PhysRevB.70.165310.
71. Côté, R.; Fertig, H.A. Collective modes of quantum Hall stripes. *Phys. Rev. B* **2000**, *62*, 1993–2007. https://doi.org/10.1103/PhysRevB.62.1993.
72. Ettouhami, A.M.; Doiron, C.B.; Klironomos, F.D.; Côté, R.; Dorsey, A.T. Anisotropic States of Two-Dimensional Electrons in High Magnetic Fields. *Phys. Rev. Lett.* **2006**, *96*, 196802. https://doi.org/10.1103/PhysRevLett.96.196802.
73. Tsuda, K.; Maeda, N.; Ishikawa, K. Anisotropic ground states of the quantum Hall system with currents. *Phys. Rev. B* **2007**, *76*, 045334. https://doi.org/10.1103/PhysRevB.76.045334.
74. Huang, Y.; Sammon, M.; Zudov, M.A.; Shklovskii, B.I. Isotropically conducting (hidden) quantum Hall stripe phases in a two-dimensional electron gas. *Phys. Rev. B* **2020**, *101*, 161302. https://doi.org/10.1103/PhysRevB.101.161302.
75. Coleridge, P.T.; Zawadzki, P.; Sachrajda, A.S. Peak values of resistivity in high-mobility quantum-Hall-effect samples. *Phys. Rev. B* **1994**, *49*, 10798–10801. https://doi.org/10.1103/PhysRevB.49.10798.
76. Ando, T. Theory of Quantum Transport in a Two-Dimensional Electron System under Magnetic Fields II. Single-Site Approximation under Strong Fields. *J. Phys. Soc. Jpn.* **1974**, *36*, 1521.
77. Daou, R.; Chang, J.; LeBoeuf, D.; Cyr-Choinière, O.; Laliberté, F.; Doiron-Leyraud, N.; Ramshaw, B.J.; Liang, R.; Bonn, D.A.; Hardy, W.N.; et al. Broken rotational symmetry in the pseudogap phase of a high-Tc superconductor. *Nature* **2010**, *463*, 519–522. https://doi.org/10.1038/nature08716.
78. Chu, J.H.; Analytis, J.G.; Greve, K.D.; McMahon, P.L.; Islam, Z.; Yamamoto, Y.; Fisher, I.R. In-Plane Resistivity Anisotropy in an Underdoped Iron Arsenide Superconductor. *Science* **2010**, *329*, 824–826, [https://www.science.org/doi/pdf/10.1126/science.1190482]. https://doi.org/10.1126/science.1190482.
79. Jin, C.; Tao, Z.; Li, T.; Xu, Y.; Tang, Y.; Zhu, J.; Liu, S.; Watanabe, K.; Taniguchi, T.; Hone, J.C.; et al. Stripe phases in WSe2/WS2 moirésuperlattices. *Nature Materials* **2021**, *20*, 940–944. https://doi.org/10.1038/s41563-021-00959-8.
80. Cao, Y.; Rodan-Legrain, D.; Park, J.M.; Yuan, N.F.Q.; Watanabe, K.; Taniguchi, T.; Fernandes, R.M.; Fu, L.; Jarillo-Herrero, P. Nematicity and competing orders in superconducting magic-angle graphene. *Science* **2021**, *372*, 264–271, [https://www.science.org/doi/pdf/10.1126/science.abc2836]. https://doi.org/10.1126/science.abc2836.